ARCHIVES
of
FOUNDRY ENGINEERING

ISSN (2299-2944)
Volume 2026
Issue 2/2026

141 – 148

17/2

10.24425/afe.2026.158000

Published quarterly as the organ of the Foundry Commission of the Polish Academy of Sciences

Does an Increase in Iron Content Affect the Shrinkage Porosity of Secondary Al-Si Alloys?

J. Piątkowski *, K. Gródek, J. Fusiarz
Faculty of Materials Engineering, Silesian University of Technology, Poland
* Corresponding author: E-mail address: jaroslaw.piatkowski@polsl.pl

Received 01.12.2025; accepted in revised form 05.03.2026; available online 14.07.2026

Abstract

This article attempts to answer the question of which theory of porosity formation in Al-Si alloy castings is correct? The one that suggests shrinkage porosity results from the presence of plate-like β-Al_5FeSi phases in the alloy, or the one that porosity is caused by thin, double-layer oxide films? The study was conducted on an AlSi7Mg alloy with an increased content of secondary materials (from 45% to 65%), gravity cast at low pressure (up to 0.15 MPa). It was shown that the main factor that determines the causes of shrinkage porosity in aluminium alloys is the method of delivering the liquid metal to the mould cavity. The microstructure examination results of the gravity-cast AlSi7Mg alloy showed that, with increasing iron content, the quantitative fraction of the β-Al_5FeSi phase increases, and their length grows from approximately 40 μm (at 0.4 wt.% Fe) to about 700 μm (at 0.8 wt.% Fe). Under such conditions, the dominant cause of shrinkage porosity in castings is the b-Fe phase, whose unfavorable morphology blocks the interdendritic alloy flow channels. This results in decreased permeability between dendrites α(Al), and consequently increased casting porosity. In pressure castings, the proportion of β-Fe phases is negligible (length up to approximately 30 μm). Numerous oxides were found in close proximity to shrinkage pores. After solidification of the AlSi7Mg alloy, these air "gaps" constitute pores that are not associated with β-Fe phases. Therefore, it can be concluded that in pressure castings, thin oxide films ("bifilms") are a more significant cause of shrinkage porosity than the β-Fe phases.

Keywords: Al-Si cast alloys, Shrinkage porosity, Microstructure of Al-Si alloys, Iron phases, Double-layer oxide films

1. Introduction

Iron is the most common and one of the most harmful impurities present in Al-Si alloys cast from secondary materials. Its influence on mechanical properties, especially ductility is particularly negative when it exceeds about 0.4 wt.% (for gravity-cast alloys) [1, 2] and 1.6 wt.% (for high-pressure die castings) [3-5]. This occurs because iron has very low solubility in the α(Al) solid solution (from 0.052% at 655°C down to 0.0052% at 450°C) [6]. For this reason, it shows a strong tendency to combine with other elements, forming intermetallic phases of various stoichiometries, structures, and sizes, among which the most undesirable is β-Al_5FeSi (the so-called β-Fe phase) [7-9]. Due to its low coherence with the matrix and its large size, it increases the brittleness of the alloy, hinders machining of castings, and reduces tensile strength [10, 11]. Additionally, the plate- or needle-like morphology of the β-Fe phase worsens the fluidity, ductility, and corrosion resistance of aluminium alloys [12]. Another important cause of reduced mechanical properties in cast aluminium alloys is porosity. According to studies [13], an increase in porosity by about 3-4% causes a decrease in tensile strength R_m by approximately 40%. The formation of porosity in aluminium and its alloys is caused by the combination of two processes [14-16]:

- the contraction of the metal during cooling of the casting, which causes a pressure drop in the liquid phase within the growth zone of α(Al) dendrites - Darcy's law [17],
- the dissolution and segregation of gaseous species(oxides, sulfides, nitrides), and particularly hydrogen, in the metal bath, occurring with varying intensity [18-20].

When the gas concentration reaches the solubility limit, decreasing with pressure and temperature micropores nucleate. These processes (homogeneous or heterogeneous) are well known and described in the literature [21-23]. These studies show that pore nucleation is mainly caused by the contact of the liquid alloy with the mould walls, by inclusions, and by the presence of gas bubbles. The chemical composition of the alloy is also important. Copper, silicon, and zinc decrease porosity; chromium, cobalt, manganese, and molybdenum have little effect on porosity; and magnesium, lithium, and titanium slightly increase porosity [24].

The type of casting process (gravity or pressure die casting) and its parameters also play an important role in the occurrence of porosity in castings, including:

- the superheating temperature of the liquid alloy above T_{liq},
- the solidification front velocity and temperature gradient,
- the solidification interval (T_{liq}–T_{sol}) and solidification time,
- refining and modification processes (e.g., with strontium or titanium with boron or phosphorus).

The influence of these factors on porosity is well known and widely described in the literature [25-28]. The reduction of gas porosity in aluminium alloys is also well documented [14, 16]. Much greater concerns arise when attempting to determine the relationship between shrinkage porosity and the presence of morphologically unfavorable iron phases in the alloy, mainly the β-Al_5FeSi phase. In general, there are two groups of theories explaining the causes of porosity formation.

The first is based on the presence of brittle, plate-like β-Fe phase precipitates in Al-Si alloys, especially when the iron content exceeds about 0.4 wt.% Fe. These phases particularly when they crystallize as primary phases block the interdendritic channels through which the melt flows, and at high Fe contents they also promote the nucleation of eutectic silicon crystals. This reduces the permeability between the α(Al) dendrites, especially the secondary ones, and consequently increases the porosity of castings [29-31].

The second theory concerns the presence of thin, two-layered oxide films, which adopt a spherical or flattened shape during casting. This is caused by turbulent metal flow, which leads to their entanglement and folding. These films, called "bifilms" by Campbell [32], have a high sintering temperature (~1900 °C) and poor wettability, especially on their folded, rough surfaces, and remain unbonded to other constituents, forming voids in the liquid. After metal solidification, these air 'fissures' form pores that are not connected to β-Fe phases. The formation of bifilms in Al-Si-Mg cast alloys has been described in studies [33].

The analysis of the considerations indicates that these theories are sometimes contradictory and do not fully explain the relationship, particularly the quantitative relationship between the β-Fe phase and/or oxide films and porosity. On this basis, it is justified to undertake further studies aimed at clarifying the causes of shrinkage porosity formation in Al-Si alloy castings with an increased share of charge scrap. This will contribute to a better understanding of the potential influence of β-Fe phases on porosity, or the lack thereof.

2. Scope and objectives of the study

The aim of the study was to determine the effect of iron content on shrinkage porosity in gravity and low-pressure castings produced from the AlSi7Mg alloy with an increased share of charge scrap. At the same time, the study sought to answer the following question: which of the theories explaining porosity formation in castings made from secondary Al-Si alloys is valid? Is it the theory that assumes shrinkage porosity results mainly from the presence of platelet-shaped β-Fe phases, which hinder the flow of the liquid alloy during solidification, or the one according to which porosity formation is caused solely by thin, double-layer oxide films?
To achieve this objective, the scope of the research included:

- the analysis of the chemical composition of AlSi7Mg alloy samples with increasing iron content, cast either by gravity casting – GC or by low-pressure casting – LPC (up to 0.15 MPa),
- microstructural investigations including quantitative and qualitative analyses of the presence of β-Fe phase precipitates in the alloy and the fraction of shrinkage porosity.

3. Research materials and methodology

The presented literature review shows that the main factor determining the causes of shrinkage porosity formation in aluminium alloys is the method by which the liquid metal is delivered to the mould cavity. Therefore, the same alloy was cast both gravitational and low pressure, and the fraction of the β-Al_5FeSi phase and shrinkage porosity in both types of castings was compared. A commercial AlSi7Mg alloy with increasing iron content, used for gravity and pressure castings mainly in the automotive and aviation industries, was selected for the study. The increase in Fe content is due to the higher share of secondary charge materials (from 45% to 65%), which consist of circulating scrap both in-house and purchased from other aluminium foundries. The scrap quality was selected to obtain the expected iron content.
Five samples with an iron content from 0.4 wt.% Fe (GC1) to 0.8 wt.% Fe (GC5) were gravity cast into a metal mould, and five samples with an iron content from 0.8 wt.% (LPC1) to 1.2 wt.% (LPC5) were low pressure cast (Fig. 1) on a Kurtz ND-GM B47 casting machine, with an average pouring velocity of approximately 0.04 $m \cdot s^{-1}$. The castings were produced at Superior Industries Production in Stalowa Wola.
A summary of all tested samples is presented in Table 1.

Table 1.
A summary of all tested samples and their casting methods

Number sample	ID sample	Approximate scrap share, wt.%[1]	Estimated scrap share, wt.%	Alloy preparation procedure	Casting method and conditions
1.	GC1	45	0.4	modification in the furnace using AlTi5B master alloy[2]; refining in the furnace using EBAH40 flux [3]	GC from a temp. of 720 °C into a steel mould, followed by solidification in air
2.	GC2	50	0.5		
3.	GC3	55	0.6		
4.	GC4	60	0.7		
5.	GC5	65	0.8		
6.	LPC1	45	0.8	Modification in the furnace using AlTi5B; refining in the ladle with nitrogen and an NH_2 mixture [4]	LPC casting from a temperature of 720 °C into an overflow ladle
7.	LPC2	50	0.9		
8.	LPC3	55	1.0		
9.	LPC4	60	1.1		
10.	LPC5	65	1.2		

where:
[1] – the remainder of the charge (up to 100%) consisted of primary materials, i.e.
pure elements, alloys, and master alloys,
[2] – AlTi5B1 master alloy (in the form of bars), 0.2 wt.% of the charge mass,
[3] – EBA H40 flux (in powder form), added at 0.05 wt.% of the charge mass.
Metalodlew, Tomaszowice near Lublin, Poland,
[4] – refining with nitrogen (99.9% purity) for 10-15 minutes, depending on the
alloy mass in the ladle, followed by refining with an NH_2 mixture (90% N +
10% H) for 3-5 minutes.

Chemical composition analysis was performed using an optical emission spectrometer for quantitative elemental analysis, the Foundry-Master Compact 01L00113 Worldwide Analytical System (Spectro Lab, Kleve, Germany). The arithmetic mean was calculated from eight measurements, and the results were rounded to two decimal places.

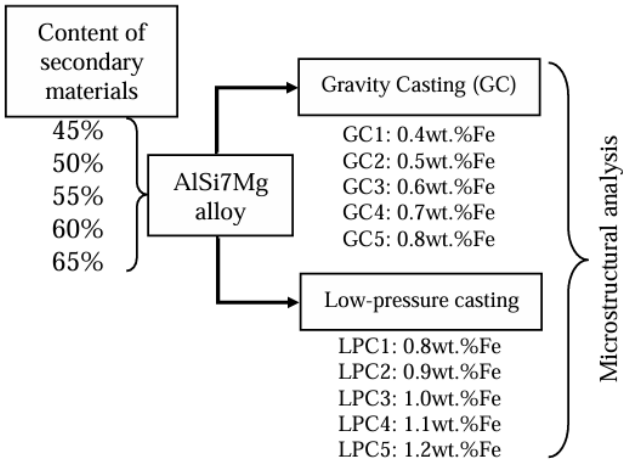

Fig. 1. Schematic of the experimental plan

LM microstructure examinations were performed using a MeF2 light microscope, and SEM analyses were carried out with a Hitachi S-3400N scanning electron microscope (Hitachi High-Technologies, Tokyo, Japan) equipped with a Thermo Noran energy-dispersive X-ray spectrometer (EDS), a Thermo MagnaRay wavelength-dispersive spectrometer (WDS), and an INCA HKL Nordlys detector for electron backscatter diffraction (EBSD).Ten photographs were taken, of which selected images are representative of the microstructure of the AlSi7Mg alloy. Some specimens were etched in Fuss's reagent.
Quantitative analysis of the microstructure was performed using quantitative metallography and image analysis with the ImageJ software [28]. For each sample, 10 photographs were taken at randomly selected fields of view. Images of the β-Fe phases were subjected to morphological transformation to correctly represent their size and shape. The measurement was carried out using the area method.

4. Test results

The chemical composition of the tested samples is presented in Table 2.

Table 2.
Chemical composition of the AlSi7Mg cast alloy*

sample number	Chemical composition, (wt.%)**						
	Si	Mg	Fe	Mn	Cu	Ni	Al
GC1	6.93	0.57	0.42	0.21	0.05	0.04	rest
GC2	7.11	0.62	0.49	0.26	0.07	0.03	rest
GC3	7.08	0.60	0.61	0.31	0.03	0.04	rest
GC4	6.96	0.59	0.71	0.35	0.03	0.02	rest
GC5	6.97	0.61	0.80	0.41	0.05	0.02	rest
LPC1	7.05	0.62	0.81	0.20	0.04	0.04	rest
LPC2	7.12	0.60	0.92	0.25	0.03	0.03	rest
LPC3	7.20	0.59	1.09	0.32	0.04	0.02	rest
LPC4	7.18	0.62	1.11	0.36	0.03	0.01	rest
LPC5	6.98	0.61	1.21	0.42	0.05	0.03	rest

* – the mean of eight measurements, after discarding the two most extreme
values,
** – up to 0.01 wt.% for the remaining elements, mainly: Zn, Na, Pb, Sr, Ti,
GC1-GC5 – designation of samples cast by gravity casting,
LPC1-LPC5 – designation of samples cast under low pressure (up to 0.15 MPa).

Representative LM microstructures of the AlSi7Mg alloy cast by gravity are shown in Figure 2, those cast under low pressure in Figure 3, and the SEM microstructures in Figure 4.

The second part of the microstructural analysis was the quantitative analysis of the β-Fe phase precipitations and the pore share fraction, as shown in Figures 5 and 6. The quantitative analysis concerned the effect of iron content on the volume fraction and length of β-Fe phases and the surface area and pore fraction, as well as the effect of the amount of β-Fe phases on the surface area and pore fraction.

The determined values are the arithmetic mean of ten measurements, after excluding the two extreme values. The dispersion of the results, measured by standard deviation (SD), is shown below Figures 5 and 6. Measurement error SD less than 0.05%.

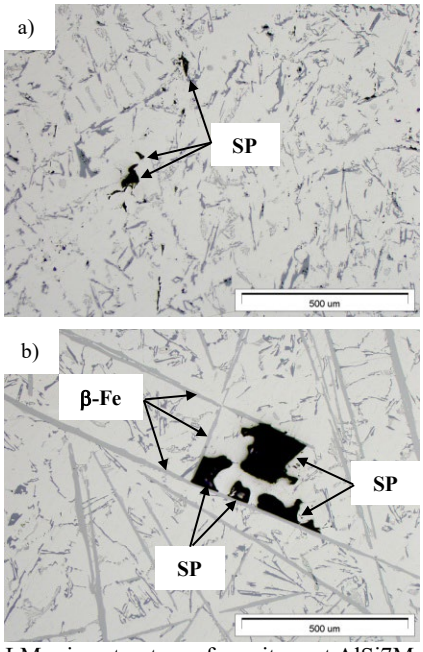

Fig. 2. LM microstructure of gravity cast AlSi7Mg alloy:
a) sample GC2 (0.49wt.%Fe);
b) sample GC5 (0.80wt.%Fe) (SP – shrinkage porosity)

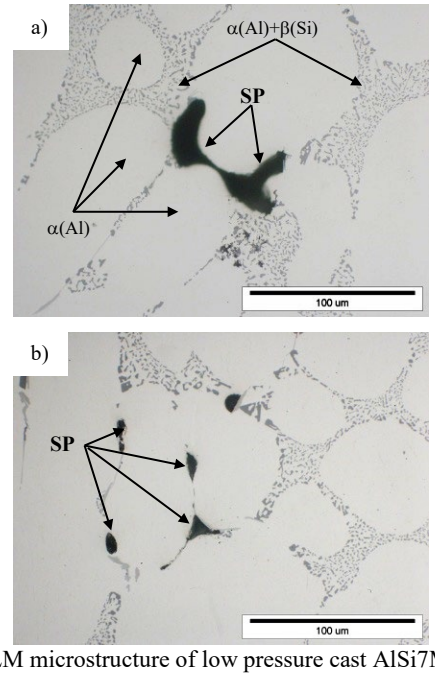

Fig. 3. LM microstructure of low pressure cast AlSi7Mg alloy:
a) sample LPC3 (1.09wt.%Fe); b) sample LPC5 (1.21wt.%Fe)
(SP – shrinkage porosity)

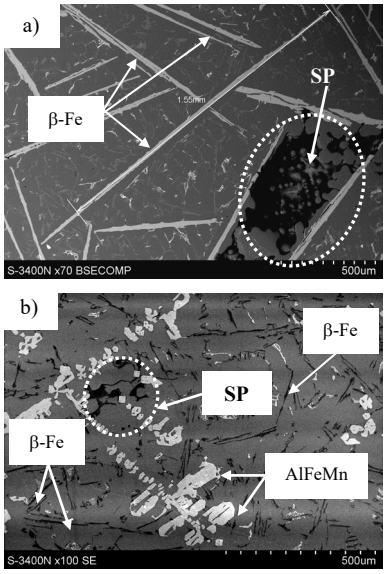

Fig. 4. SEM microstructure of AlSi7Mg alloy: a) gravity cast (sample GC5); b) low pressure cast (sample LPC5)

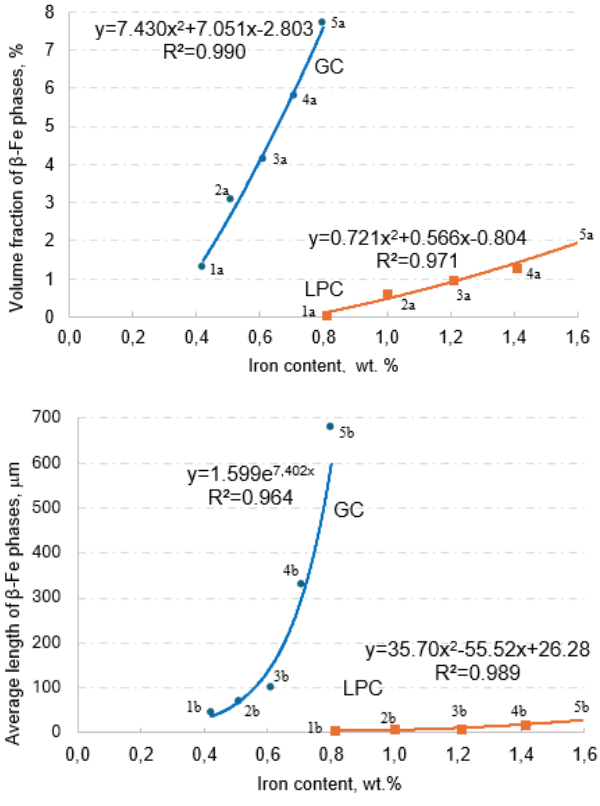

Point number	1a/1b	2a/2b	3a/3b	4a/4b	5a/5b
SD for GC	0.022/3.27	0.09/4.11	0.26/4.31	0.35/9.39	0.48/14.52
SD for LPC	0.010/0.012	0.011/0.011	0.013/0.012	0.011/0.011	0.012/0.011

Fig. 5. Change in: a) the mean volume of β-Al5FeSi phase; b) the length of β-Al5FeSi phase as a function of iron content in the AlSi7Mg alloy cast by GC and by LPC

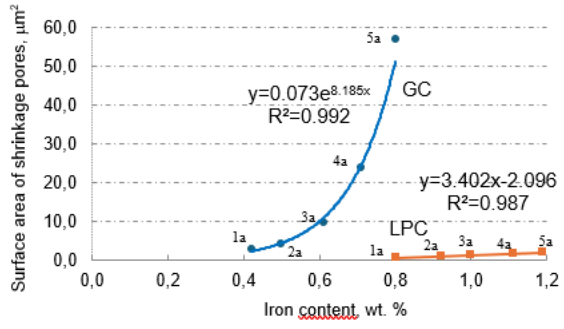

a)

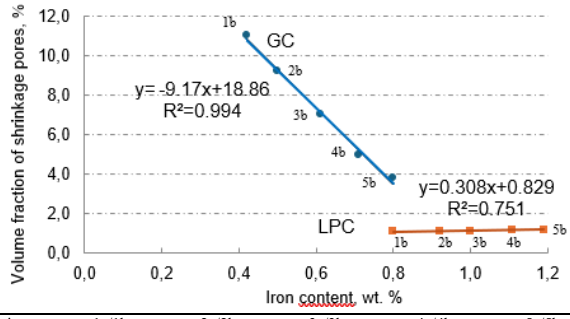

b)

Point number	1a/1b	2a/2b	3a/3b	4a/4b	5a/5b
SD for GC	0.021/2.711	0.034/1.66	0.42/1.05	0.91/0.82	2.48/0.55
SD for LPC	0.016/0.012	0.016/0.011	0.018/0.012	0.021/0.011	0.022/0.010

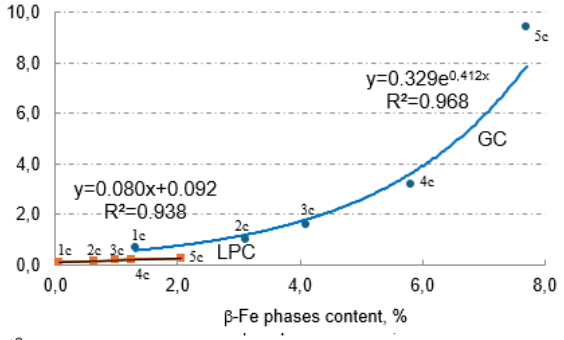

c)

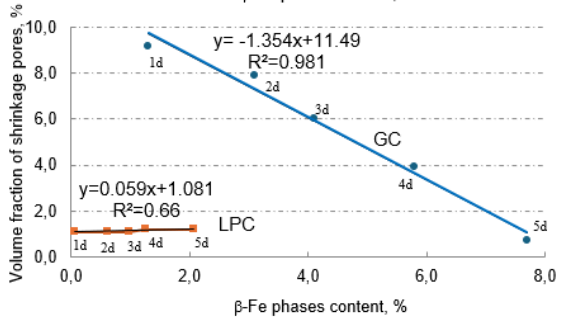

d)

Point number	1c/1d	2c/2d	3c/3d	4c/4d	5c/5d
SD for GC	0.021/0.026	0.079/0.14	0.22/0.30	0.33/0.36	0.48/0.50
SD for LPC	0.011/0.011	0.013/0.010	0.011/0.010	0.010/0.010	0.011/0.010

Fig. 6. The influence of iron content on: a) surface area; b) volume fraction and the content of β-Fe phases on: c) surface area; d) volume fraction of shrinkage pores in the AlSi7Mg cast alloy

5. Discussion of results

The aim of the study was to determine whether the increasing iron content, resulting from the higher proportion of secondary materials (from 45% to 65%), affects shrinkage porosity. A secondary objective was therefore, to attempt to answer the question: which of the theories of porosity formation in Al-Si alloy castings is correct? The one that suggests shrinkage porosity results from the presence of platelet-shaped β-Fe phases in the alloy, which hinder the free access of liquid metal to interdendritic regions during solidification [29-31], or the one according to which the main cause of shrinkage porosity is thin, double-layer oxide films, on which iron phases may possibly form [32, 33]? The second part of the microstructural study focused on the quantitative analysis of the β-Fe phase fraction and shrinkage porosity in gravity and low pressure cast AlSi7Mg alloy (up to 0.15 MPa).

The literature review showed that the main factor determining the causes of shrinkage porosity formation in aluminium alloys is the method by which the liquid metal is delivered into the mould cavity. Therefore, the AlSi7Mg alloy was cast both by gravity casting (GC) and low pressure casting (LPC), and then, using LM and SEM metallographic examinations, the microstructures were compared with respect to the fraction of the β-Al5FeSi phase (volume fraction and average length) and shrinkage porosity (pore surface area and pore fraction).

The microstructural examination results of the gravity cast AlSi7Mg alloy showed that, with increasing iron content, the quantitative fraction of the β-Al5FeSi phase increases, and their length grows from approximately 40 µm (at 0.4 wt.% Fe) to about 700 µm (at 0.8 wt.% Fe) (Fig. 2b). Such a significant increase in the length of the plate-like β-Fe phase precipitates is caused by the sequence of their crystallization relative to the other constituents of the Al-Si alloy structure. As studies have shown [34], up to about 0.4 wt.% Fe, the β-Fe phases form after the crystallization of the α(Al)+β(Si) eutectic or during it, and their length averages from 40 to 80 µm. At iron contents from 0.41 to about 0.69 wt.% Fe, the β-Fe phases (with an average length of 80 - 400 µm) form before the α(Al)+β(Si) eutectic and after the α(Al) solid-solution dendrites. At iron contents above 0.7 wt.% Fe, the β-Fe phases solidify as primary crystals, and therefore their length is the greatest on average from 500 to 700 µm, and sometimes even up to 1.2 mm (Fig. 4a). Plate-like β-Fe phases that form primarily (without any obstacles) at the solidification front hinder the flow of liquid metal into the α(Al) interdendritic regions, and the resulting voids form shrinkage pores upon solidification (Fig. 2b). Therefore, in Al-Si secondary alloys with increasing iron content, it is highly probable that shrinkage porosity forms as a result of the crystallization of β-Fe phases, which block the interdendritic flow channels of the alloy. This is especially evident at iron contents above 0.7 wt.% Fe, which reduces the permeability between α(Al) dendrites and consequently increases shrinkage porosity in Al-Si alloy castings.

These results are consistent with the studies [23, 29], which showed that, with increasing iron content, the fraction of β-Al5FeSi phases increases, and consequently, clusters of shrinkage porosity become more pronounced. The author of the study [29] also states that such a situation negatively affects the mechanical properties of the castings, and therefore it is necessary to add, for example, manganese to Al–Si alloys with increased iron content.Similar conclusions can be drawn from the studies [7, 12, 14-16], which

indicate that the porosity of Al-Si alloys results from an increase in iron content.

The second part of the microstructure study involved a quantitative analysis of the β-Fe phase content and shrinkage porosity in the AlSi7Mg alloy cast by gravity and low-pressure casting (up to 0.15 MPa). Figure 5 shows that increasing iron content increases the β-Fe phase content and average length only for GC (from 0.4 wt.% to 0.8 wt.% Fe). In the case of LPC, no significant increase in the β-Fe phase content, as measured by their surface area and length, was observed. However, the microstructures of the tested pressure-cast alloy indicate the presence of shrinkage pores (Figs. 3 and 4a). This is confirmed by our own research [28, 34]. It is true that in the AlSi7Mg alloy cast in the LPC process the presence of plate-like β-Fe phase precipitates was also found, but their share is small and the average length does not exceed approximately 20 μm (Fig.4b).

As shown in Fig. 5, increasing the iron content causes an increase in both the fraction and the average length of β-Fe phases, but only for gravity cast samples (from 0.4 wt.% to 0.8 wt.% Fe). In the case of low pressure castings, no significant increase in the fraction of β-Fe phases, measured by their surface area and length, was observed. As shown in Figures 6a and 6b, in gravity cast samples, an increase in iron content leads to an increase in the surface area of shrinkage pores and a decrease in their fraction, i.e., the number of pores decreases while their size increases. In contrast, in low-pressure castings, both the pore surface area and their fraction remain relatively constant. Therefore, it may be concluded that iron content has only a minor effect on the formation of shrinkage porosity in low pressure castings. This is also confirmed by the results presented in Figures 6c and 6d. In gravity cast samples, an increase in the fraction of β-Fe phases is accompanied by an increase in the size of shrinkage pores (expressed by their surface area), while their number decreases. In low pressure castings the influence of β-Fe phases on shrinkage porosity is minor.

Microstructural analysis shows that, in the pressure-cast AlSi7Mg alloy, oxides are the main source of porosity. They most commonly form during the pouring of the alloy from the furnace to the ladle or from the furnace to the mould, as confirmed by studies [8, 9, 25]. According to Campbell, although aluminium alloys are prone to oxide formation (liquid aluminium has a strong affinity for oxygen) and oxidation occurs within milliseconds when the aluminium surface comes into contact with atmospheric oxygen and moisture, the top of the liquid AlSi7Mg alloy forms a compact surface that prevents gases from penetrating into the alloy. Therefore, it is crucial to minimize alloy pouring and, in particular, turbulence of the liquid metal during the first and second stages of pressure casting. Accordingly, a low ram movement speed (in the first stage) and low filling pressure of the mould cavity (in the second stage) are recommended. This is confirmed by studies [4, 13, 18, 33] for example. Therefore, it can be stated that in pressure-cast alloys, which are exposed to pouring and turbulence in the liquid state, the more probable theory regarding the causes of shrinkage porosity is the presence of flat, double oxide films in the alloy rather than the morphologically unfavorable β-Al_5FeSi phases.

6. Conclusions

In summary, it can be stated that some of the most important factors determining the causes of shrinkage porosity in aluminium alloys are the casting method (gravity or pressure), the iron content and the amount of gaseous impurities, especially oxygen and hydrogen.

In gravity-cast Al-Si-Mg alloys with an iron content of up to about 0.4 wt.% Fe, the β-Al_5FeSi phases do not pose a major problem, and therefore porosity is often accepted by customers. With an iron content from 0.41 to about 0.69 wt.% Fe, the β-Al_5FeSi phases (with an average length of 80-400 μm) form before the α(Al)+β(Si) eutectic. In this case, isolated clusters of shrinkage porosity begin to appear, but they are not yet very large, because dendrites of the α(Al) solid solution have already formed earlier, effectively limiting the growth of the β-Fe phases. With an iron content above 0.7 wt.% Fe, the β-Fe phases crystallize primarily, and therefore their length is the greatest, as they can grow freely without encountering any 'obstacles'. In this case, the primary β-Al_5FeSi phases completely block the free flow of the liquid alloy, causing large clusters of shrinkage porosity whose morphology reflects the shape of the subsequently crystallizing α(Al) solid-solution dendrites. Then, it becomes necessary to introduce manganese- or chromium-based master alloys into the melt [4, 7, 22]. These elements, due to the similarity of their crystallographic parameters to iron, cause the plate-like β-Al_5FeSi phases to transform into phases of the $Al_X(Fe,Mn,Cr)_YSi_Z$ type [8, 9, 12].

In view of the above, the main cause of shrinkage porosity formation in gravity-cast Al-Si-Mg alloys is the presence of iron phases, among which the β-Al_5FeSi phase is the most detrimental. The contribution of oxide impurities is insignificant.

In the case of pressure-cast Al-Si-Mg alloys, the presence of β-Fe phases is not as harmful, and therefore a higher iron content is acceptable. The rapid solidification of pressure-cast parts in permanent moulds prevents the β-Fe phases from reaching sizes large enough to obstruct the flow of liquid alloy at the solidification front. However, a problem arises from the necessity to transfer the alloy from the furnace to the ladle (where refining takes place) and subsequently from the ladle to the low-pressure casting machine. However, a problem arises from the necessity to transfer the alloy from the furnace to the ladle (where refining takes place) and subsequently from the ladle to the low pressure casting machine. This may lead to the unfavourable phenomenon of air entrapment [35], resulting in the formation of oxide films.

It should be noted, however, that due to the very small size of oxide films, their identification is extremely difficult.This requires specialized research equipment and 3D scanning methods at the micrometric scale, followed by a laborious process of identifying these films. Consequently, the most effective method for identifying the causes of shrinkage pore formation and their presence in the microstructure of Al–Si alloys is quantitative metallographic analysis.

On this basis, it can be stated that in the tested low pressure cast alloy, the main source of porosity is not the plate-like β-Fe precipitates, but oxides which, due to their double-layer structure, are referred to by Campbell as 'bifilms'. Therefore, in the case of pressure-cast Al-Si alloys, the theory that porosity forms due to the presence of oxides in the alloy is more likely. In this case, master alloys (e.g., manganese- and/or chromium-based) are also added;

however, care must be taken not to exceed the allowable values of the so-called 'sludge factor,' which is highly undesirable due to the presence of hard particles rich mainly in iron, manganese, and chromium [3, 4, 10, 11, 18].

Acknowledgments

The authors wish to express their sincere thanks to the management of Superior Industries Production of Poland in Stalowa Wola for providing the research materials and for their support in the preparation of this publication.

References

[1] Kammer, C. (2011). *Aluminium Handbook. Vol. 1: Fundamentals and Materials*. Berlin: Beuth Verlag GmbH.

[2] Mbuya, T.O., Odera, B.O. & Ng'ang'a, P.S. (2003). Influence of iron on castability and properties of Al-Si alloys: literature review. *International Journal of Cast Metals Research*. 16(5), 451-465. https://doi.org/10.1080/13640461.2003.11819622.

[3] Ferraro, S., Fabrizi, A. & Timelli, G. (2015). Evolution of sludge particles in secondary die-cast Al alloys as function of Fe, Mn, Cr contents. *Materials Chemistry and Physics*. 153, 168-179. https://doi.org/10.1016/j.matchemphys.2014.12.050.

[4] Seifedine, S. & Svensson, I.L. (2009). The influence of Fe and Mn content and cooling rate on the microstructure and mechanical properties of A380-die casting alloys. *Metallurgical Science and Technology.* 27-1, 11-20. https://www.fracturae.com/index.php/MST/issue/view/247.

[5] Piątkowski, J. & Chowaniec, L. (2025). Effect of scrap on microstructure and mechanical properties of ENAB-42000 alloy pressure die castings. *Journal of Physics: Conference Series*. 3035(1), 012019, 1-10. DOI:10.1088/1742-6596/3035/1/012019.

[6] Belov, N.A., Aksenov, A.A., Eskin, D.G. (2002). *Iron in Aluminum Alloys. Impurity and Alloying Element*. London: CRC Press. https://doi.org/10.1201/9781482265019.

[7] Ebhota, W. S., & Jen, T.-C. (2018). Intermetallics formation and their effect on mechanical properties of Al-Si-X alloys. In M. Aliofkhazraei (Eds.), *Intermetallic Compounds – Formation and Applications*. IntechOpen. https://doi.org/10.5772/intechopen.73188.

[8] Mahta, M., Emamy, M., Cao, X. & Campbell, J. (2008). Overview of β-Al_5FeSi phase in Al-Si cast alloys. *Materials Science Research Trends.* 251-271. https://nrc-publications.canada.ca/eng/view/accepted/?id=62793dff-84af-4087-b2c1-4011e84b04a2.

[9] Cao, X. & Campbell, J. (2006). Morphology of β-Al_5FeSi phase in Al-Si cast alloys. *Materials Transactions*. 47(5), 1303-1312. https://doi.org/10.2320/matertrans.47.1303.

[10] Khalifa, W, Samuel, F.H. & Gruzleski, J.E. (2003). Iron intermetallic phases in the Al corner of the Al-Si-Fe system. *Metallurgical and Materials Transactions*. 34(13), 807-825. https://doi.org/10.1007/s11661-003-1009-9.

[11] Mikołajczyk, P. & Ratke, L. (2015). Three dimensional morphology of β-Al_5FeSi intermetallics in AlSi alloys. *Archives of Foundry Engineering.* 15(1), 47-50.

[12] Lu, L. & Dahle, A.K. (2005). Iron-rich intermetallic phases and their role in casting defect formation in hypoeutectic Al-Si alloys. *Metallurgical and Materials Transactions.* 36A, 819-835. https://doi.org/10.1007/s11661-005-1012-4.

[13] Cais, J., Weiss, V. & Svobodova, J. (2014). Relation between porosity and mechanical properties of al-si alloys produced by low-pressure casting. *Archives of Foundry Engineering*. 14(spec.1), 97-102. ISSN (1897-3310).

[14] Elwin, L. & Rooy, E. (1992). Mechanisms of porosity formation in aluminum. *Modern Casting*. 82, 34-36.

[15] Sigworth, G. & Wang Ch. (1993). Mechanisms of porosity formation during solidification: A theoretical analysis. *Metallurgical and Materials Transactions.* 24(2), 349-364. https://doi.org/10.1007/BF02659138.

[16] Monroe, R. (2012). Porosity in Castings. *AFS Transactions*. 205(4), 205-245. https://doi.org/10.1002/chin.200642218.

[17] Peaceman, D.W. (1977). *Fundamentals of numerical reservoir simulation*. Elsevier.

[18] Guo, H.M., Yang, X.J. & Wang, J.X. (2009). Pressurized solidification of semi-solid aluminum die casting alloy A356. *Journal of Alloys and Compounds*. 485(1-2), 812-816. https://doi.org/10.1016/j.jallcom.2009.06.083.

[19] Agnes, M.S., Ehab S., Songmene V. & Fawzy H.S. (2023). Review on porosity formation in aluminum alloys. *Materials*. 16(5), 2047, 1-26. https://doi.org/10.3390/ma16052047.

[20] Kent, D. Carlson, Zhiping, Lin, Cchristoph, Beckermann (2007). Modeling the effect of finite-rate hydrogen diffusion on porosity formation in aluminum alloys. *Metallurgical and Materials Transactions*. 38B, 541-555. DOI: 10.1007/s11663-006-9013-2.

[21] Ambat, R. & Dwarakadasa E.S. (1990). Effect of hydrogen in aluminium and aluminium alloys: A review. *Materials Science*. 19(1), 103-114. http://doi.org/10.1007/BF02744792.

[22] Samuel, A., Zedan, Y., Doty, H., Songmene, V. & Samuel, F.H. (2021). Overview of the main sources of porosity in Al-Si cast alloys. *Advances in Materials Science and Engineering*. 21(1), 1-16. https://doi.org/10.1155/2021/1921603.

[23] Tiedje, N.S., Taylor, J.A. & Easton M.A. (2013). A new multi-zone model for porosity distribution in Al-Si alloy castings. *Acta Materialia*. 61, 3037-3049. http://doi.org/10.1016/j.actamat.2013.01.064.

[24] Anyalebechi, P.N. (2013). Hydrogen-induced gas porosity formation in Al-4.5%Cu-1.4%Mg alloy. *Journal of Materials Science*. 48, 5342-5353. http://doi.org/10.1007/s10853-013-7329-2.

[25] Campbell, J. & Tiryakioglu, M. (2010). Review of effect of P and Sr modification and porosity development in Al-Si alloys. *Material Science of Technology*. 26, 262-268. http://doi.org/10.1179/174328409X425227.

[26] Gagnon, D., Samuel, A.M., Samuel, F.H., Abdelaziz, M.H., Doty, H.W. (2021). Melt treatment-porosity formation relationship in Al-Si cast alloys. *Casting Processes and Modelling of Metallic Materials*. London, UK: Intech Open. https://doi.org/10.5772/intechopen. 94595.

[27] Mohamed, A.M.A., Samuel, E., Zedan, Y., Samuel, A.M., Doty H.W. & Samuel F.H. (2022). Intermetallics formation during solidification of AlSiCuMg cast alloys. *Materials*. 15(4), 1335, 1-24. http://doi.org/10.3390/ma15041335.
[28] Piątkowski, J., Roskosz, S. & Stach, S. (2024). The influence of selected high – pressure die casting parameters on the porosity of ENAB-46000 alloy castings. *Materials*. 18(5), 361-371. https://doi.org/10.12913/22998624/191236.
[29] Taylor, J.A. (2004). The effect of iron in Al-Si casting alloys. In Proceedings of the 35th Australian Foundry Institute National Conference (pp. 148–157). Australian Foundry Institute.
[30] Sigworth, G., Campbell, J. & Jorstad J. (2009). The modification of Al-Si casting alloys: important practical and theoretical aspects. *International Journal of Metalcasting*. 3, 65-78. https://doi.org/10.1007/BF03355442.
[31] Taylor J.A., Schaffer G.B. & StJohn D.H. (1999). The role of iron in the formation of porosity in Al-Si-Cu based casting alloys: Part I. Initial experimental observations. *Metallurgical and Materials Transactions*. 30A, 1643-1650. https://linf.springer.com/article/10.1007/s11661-999-0101-1.
[32] Campbell, J. (2015*). Complete Casting Handbook: Metal Casting Processes*, *Metallurgy, Techniques and Design*. 2nd edition. Oxford: Butterworth-Heinemann.
[33] Park, J. M. (2009). *Behaviours of bifilms in A356 alloy during solidification: Developing observation techniques with 3-D micro X-ray tomography*. School of Metallurgy and Materials College of Engineering University of Birmingham. https://etheses.bham.ac.uk/id/eprint/745/1/Park10Mres.pdf.
[34] Piątkowski, J. Chowaniec, L. & Matuła, T. (2025). Application of thermal-derivative analysis to study phase transformation in AlSi7Mg alloy with different iron content. *Machines. Technologies. Materials*. 19(3), 110-113. https://stumejournals.com/journals/mtm/2025/3/110.full.pdf.